

Symmetry and structure of carbon-nitrogen complexes in gallium arsenide from infrared spectroscopy and first-principles calculations

Christopher Künneth,^{1, a)} Simon Kölbl,¹ Hans Edwin Wagner,¹ Volker Häublein,² Alfred Kersch,^{1, b)} and Hans Christian Alt^{1, c)}

¹⁾ *Munich University of Applied Sciences, Department of Applied Sciences and Mechatronics, Lothstr. 34, D-80335 Munich, Germany*

²⁾ *Fraunhofer Institute for Integrated Systems and Device Technology IISB, Schottkystrasse 10, 91058 Erlangen, Germany*

(Dated: 9 August 2021)

Molecular-like carbon-nitrogen complexes in GaAs are investigated both experimentally and theoretically. Two characteristic high-frequency stretching modes at 1973 and 2060 cm^{-1} , detected by Fourier transform infrared absorption (FTIR) spectroscopy, appear in carbon- and nitrogen-implanted and annealed layers. From isotopic substitution it is deduced that the chemical composition of the underlying complexes is CN_2 and C_2N , respectively. Piezospectroscopic FTIR measurements reveal that both centers have tetragonal symmetry. For density functional theory (DFT) calculations linear entities are substituted for the As anion, with the axis oriented along the $\langle 100 \rangle$ direction, in accordance with the experimentally ascertained symmetry. The DFT calculations support the stability of linear N-C-N and C-C-N complexes in the GaAs host crystal in the charge states ranging from +3 to -3. The valence bonds of the complexes are analyzed using molecular-like orbitals from DFT. It turns out that internal bonds and bonds to the lattice are essentially independent of the charge state. The calculated vibrational mode frequencies are close to the experimental values and reproduce precisely the isotopic mass splitting from FTIR experiments. Finally, the formation energies show that under thermodynamic equilibrium CN_2 is more stable than C_2N .

Keywords: GaAs, defects, carbon, nitrogen, semiconductors, infrared spectroscopy, first principles, DFT

I. INTRODUCTION

Carbon and nitrogen are important light-element impurities in GaAs bulk crystals as well as in GaAs-based epitaxial layers. Carbon as a common substitutional acceptor (C_{As}) is used in semi-insulating GaAs crystals to stabilize the Fermi level near the mid gap position¹. Carbon is also widely employed to grow highly p-type doped epitaxial layers^{2,3}. In the last couple of decades, the behavior of nitrogen in GaAs has attracted much interest in the context of dilute nitrides. The ternary system $\text{GaAs}_{1-x}\text{N}_x$, where a small amount x of the anion sites is replaced by the isovalent N atom, is in the focus of intense research. Addition of nitrogen to GaAs during epitaxial growth leads to a remarkable shrinkage of the band gap with an initial slope of about 180 meV for 1% ($x = 0.01$) of nitrogen⁴. This opens up the possibility of band gap engineering for example for highly efficient multi-junction solar cells⁵. Furthermore, the reversal of the band gap shrinkage by hydrogen passivation has been observed and studied theoretically⁶.

Complexes of carbon and nitrogen have an influence on these doping-related material properties. The first report of such a complex was given by Ulrici and Clerjaud⁷ in 2005. They observed a sharp local vibrational mode (LVM) at 2087.1 cm^{-1} at 7 K in the related semiconduc-

tor gallium phosphide. From the detection of small satellite bands caused by the natural isotopes ^{13}C and ^{15}N , the assignment to a CN complex was straightforward. Furthermore, uniaxial stress measurements showed that the defect has tetragonal symmetry with the carbon-nitrogen bond aligned along the $\langle 100 \rangle$ axis of the crystal. They give also a short note on a band at 2088.5 cm^{-1} in one particular GaAs crystal doped with both carbon and nitrogen. From the nearly identical vibrational frequency and similar temperature dependence as in GaP case they tentatively suggest an analogous defect in GaAs. However, in the course of this and the extensive previous study on bulk GaAs crystals this band was not observed^{8,9}.

Another carbon-related band in GaAs appears at 2059.6 cm^{-1} at 7 K¹⁰. It was first tentatively attributed to a center involving carbon and oxygen, but its origin is a carbon-nitrogen complex. The band can be observed in carbon-rich GaAs crystals after long-term annealing at around 700 °C. The intensity of the band increases with the carbon concentration as determined by the C_{As} LVM at 582 cm^{-1} . The participation of carbon in the complex is ascertained by the existence of a small ^{13}C satellite at 2003.8 cm^{-1} . From its relative intensity, the incorporation of precisely one C atom can be inferred. Furthermore, from the strength of the main band and the decrease of the substitutional carbon concentration, it can be concluded that a considerable fraction of the carbon impurities is transformed to this complex during annealing¹⁰.

Contrary to carbon, the role of nitrogen in this complex was more difficult to assess. Nitrogen as a substi-

^{a)}Electronic mail: kuenneth@hm.edu

^{b)}Electronic mail: akersch@hm.edu

^{c)}Electronic mail: hchalt@hm.edu

tutional isoelectronic impurity (N_{As}) in bulk GaAs can only be detected by mass spectrometry or LVM absorption for concentrations above 10^{15} cm^{-3} not far from the maximum doping level of some 10^{16} cm^{-3} .¹¹ Usually, the nitrogen contamination coming from the pyrolytic boron nitride crucible and the nitrogen atmosphere during crystal growth is much lower. The verification of nitrogen incorporation was carried out by some of the present authors using GaAs samples implanted with ^{12}C and the nitrogen isotopes ^{14}N and ^{15}N .⁸ In this case, high concentrations of carbon-nitrogen complexes responsible for the 2060 cm^{-1} absorption band are generated in a near-surface layer. The isotope splitting in samples implanted with both ^{14}N and ^{15}N allows the identification of the chemical composition of the complex as $[\text{CN}_2]_{As}$. Furthermore, in the same layer structures a second LVM band at 1973 cm^{-1} was found originating from another defect related to carbon and nitrogen. In contrast to $[\text{CN}_2]_{As}$, this second center contains only one N atom. So far, no further information was available.

Carbon-nitrogen complexes in GaAs and GaP were studied theoretically by Limpijumng et al.¹² based on density functional theory (DFT) calculations. Considering the carbon-nitrogen molecule in different charge states they found that in general the substitutional configuration on the anion site $[\text{CN}]_{As}$ is energetically more favorable than the interstitial one $[\text{CN}]_i$. The stretching frequency has a strong dependence on the charge state of the molecule. Only the 2+ charge state has a frequency high enough to be compatible with the experimental value found in GaP⁷. However, this charge state relaxes from the substitutional site with tetragonal symmetry to a low-symmetry off-center position contradicting the experimental result.

The present work completes previous FTIR studies by piezospectroscopic experiments for both centers in samples with surface-implanted layers (Subsections III A and III B). In Subsection III C experimental results are used as starting configurations for extensive DFT calculations and analyses of the LVM frequencies. In Subsection III D a Kohn-Sham (KS) orbital interpretation of the related eigenstates is presented and in Subsection III E the formation energies of the $[\text{CN}_2]_{As}$ and $[\text{C}_2\text{N}]_{As}$ defect.

II. EXPERIMENTAL AND COMPUTATIONAL METHODS

Single-crystalline GaAs containing carbon-nitrogen complexes in high concentration in a near-surface layer was produced by implantation of carbon and nitrogen into 5 mm thick semi-insulating wafers with $\{100\}$ or $\{110\}$ surface orientation. The total implantation dose was $5 \times 10^{15} \text{ cm}^{-2}$ for both nitrogen and carbon. Different ion energies up to 200 keV were used to obtain a roughly uniform concentration depth profile. FTIR samples were cut from this material and treated by rapid thermal annealing (RTA) at 700°C for 60 s under nitro-

gen atmosphere. Infrared (IR) absorption measurements were carried out with a Bruker Vertex 80v FTIR vacuum spectrometer equipped with a global source, a KBr beam splitter and a MCT detector. The samples were cooled to 77 K or 9 K in an optical cryostat. The implanted layer was aligned perpendicular to the IR light beam in order to get a maximum signal from the carbon-nitrogen centers. For piezospectroscopic investigations, samples with approximate dimensions of $20 \times 5 \times 5 \text{ mm}^3$ were prepared with the long axis oriented along the main crystallographic directions $\langle 100 \rangle$, $\langle 110 \rangle$, or $\langle 111 \rangle$. Uniaxial stress was applied to the sample along the long axis by a push rod coupled to a pneumatic cylinder using a home-made apparatus. The force on the sample was calculated from the gas pressure in the cylinder that was monitored on a precision gauge.

Numerical results were obtained with the all-electron DFT code FHI-Aims¹³⁻¹⁷ which utilizes numerical atom-centered basis function. The LDA (PW¹⁸ parameterization) or HSE06¹⁹ approximation with the mixing parameter $\alpha = 0.25$ and $\omega = 0.11a_0^{-1}$ was chosen as the exchange-correlation functional. All calculations are based on a 64 atoms supercell of a GaAs crystal with the cubic $F\bar{4}3m$ (No. 216) symmetry. Since FHI-Aims does not include symmetry considerations, all convergences were archived without symmetry constraints. The supercell of the defect structures $[\text{CN}_2]_{As}$ ($\text{Ga}_{32}\text{As}_{31}\text{C}_1\text{N}_2$) and $[\text{C}_2\text{N}]_{As}$ ($\text{Ga}_{32}\text{As}_{31}\text{C}_2\text{N}_1$) contains 66 atoms. A convergence study reveals that a k-point grid of $3 \times 3 \times 3$ with an electronic force convergence of $5 \times 10^{-5} \text{ eV/\AA}$ with the tight basis set in the second tier is sufficient. The unit cell and ion positions were converged for all supercells up to $5 \times 10^{-4} \text{ eV/\AA}$ except for charged cells where only ions were allowed to move keeping the unit cell as the neutral ones. Vibrational frequencies were carried out with the utility Phonopy²⁰ using finite displacements. The structural relaxation and the vibrational frequencies in this work were calculated using LDA.

Formation energies were calculated according to²¹

$$E^f[X^q] = E_{\text{tot}}[X^q] - E_{\text{tot}}[\text{GaAs}] - \sum_i n_i \mu_i + q(E_F + E_{\text{VBM}}[\text{GaAs}] + \Delta V[X^0]) + E_{\text{corr}}[X^q] \quad (1)$$

with E^f the formation energy, E_{tot} the total energy, n_i the numbers of impurities, μ_i the chemical potential of the impurity i , E_F the Fermi level referenced to the energy of the valence band maximum E_{VBM} , ΔV the potential alignment, E_{corr} the charge correction due to finite size of the unit cell and $X \in \{[\text{C}_2\text{N}]_{As}, [\text{CN}_2]_{As}\}$ the defect. Calculations for charged structures were carried out for the charges $q = -3, \dots, +3$ for both defects with the cell fixed to the uncharged structure. For $[\text{CN}_2]_{As}$ and $[\text{C}_2\text{N}]_{As}$ the chemical potential were $\sum_i n_i \mu_i = -\mu_{As} + \mu_C + 2\mu_N$ and $\sum_i n_i \mu_i = -\mu_{As} + 2\mu_C + \mu_N$, respectively. μ_{As} was calculated from trigonal arsenic, μ_C from diamond and μ_N from a N_2 molecule. Figures of

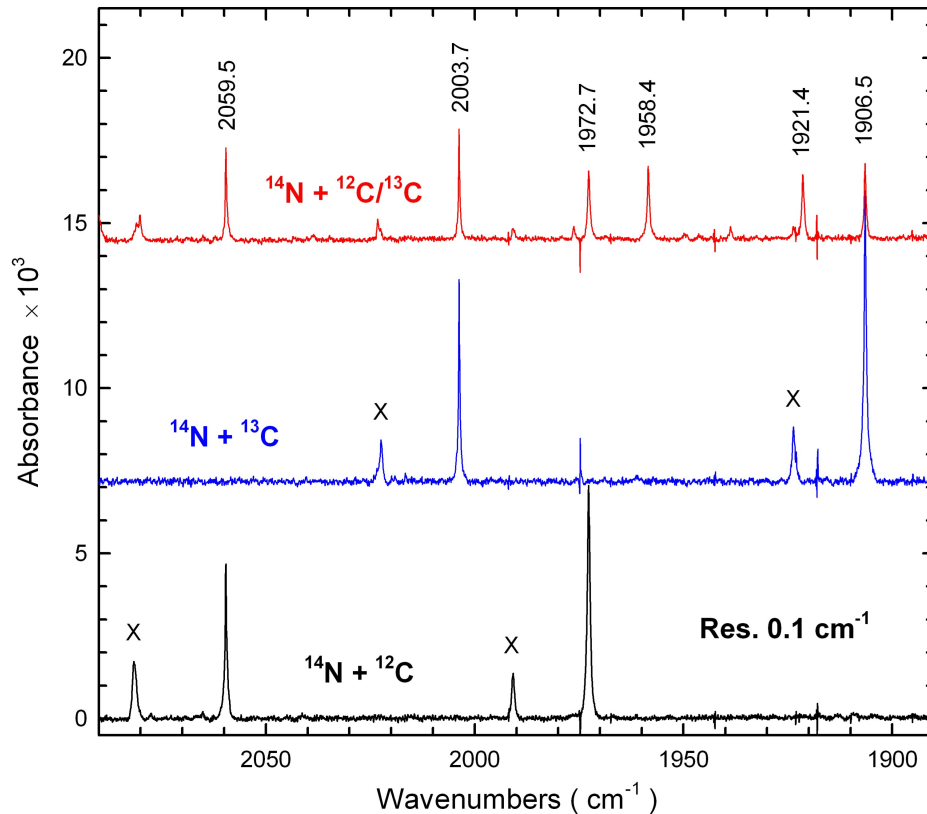


FIG. 1. Infrared absorption spectra of carbon-nitrogen related vibrational modes in GaAs at 9K after implantation of ^{14}N and ^{12}C and/or ^{13}C and annealing at 700°C . Spectra are baseline-corrected and shifted vertically for clarity. Bands marked by 'X' appear only in implanted samples and are most probably due to defects involving residual irradiation damage.

atomic structures and densities used in this publication were produced with VESTA²².

III. RESULTS AND DISCUSSION

A. Isotope shifted satellite bands

The chemical composition of the carbon-nitrogen complexes giving rise to the absorption bands at 1973 and 2060 cm^{-1} can be deduced from the characteristic mass-induced shift after isotopic substitution. As has been pointed out in Ref. 9, the replacement of ^{14}N by ^{15}N unambiguously leads to the conclusion that the former center contains one nitrogen atom, whereas the latter two in equivalent positions (configuration N-C-N). Here, we show the analogue experiment with the isotope pair ^{12}C and ^{13}C . Sample spectra at 9K after RTA at 700°C are shown in FIG. 1.

Replacement of ^{12}C by ^{13}C shifts the 2060 cm^{-1} band to 2004 cm^{-1} and the 1973 cm^{-1} band to 1907 cm^{-1} ²³. The band at 2004 cm^{-1} was first detected by Ulrici and Jurisch¹⁰ as a small satellite in carbon-doped bulk crystals caused by the naturally occurring ^{13}C isotope (natural abundance 1.1%). It should be emphasized that for both bands the shift is larger than expected from a simple bi-atomic molecule. For the mixed-isotope implantation with ^{12}C

and ^{13}C in the ratio 1:1, additional lines at 1921 and 1958 cm^{-1} appear, see upper spectrum in FIG. 1. These lines belong to the 1973 cm^{-1} defect and require that more than one C atom must be involved. The existence of four lines of equal intensity suggests that two C atoms on in-equivalent sites are incorporated called A and B. The simple statistical consideration that A and B are occupied with a probability of 50% by ^{12}C or ^{13}C brings about this result. Therefore, the chemical composition of the defect responsible for the 1973 cm^{-1} band is $[\text{C}_2\text{N}]_{\text{As}}$ (configuration C-C-N).

B. Uniaxial stress experiments

FIG. 2 illustrates the characteristics of the 1973 cm^{-1} band under uniaxial stress. For stress along a $\langle 111 \rangle$ direction the band shifts to higher energy but does not split. In contrast, stress along the $\langle 100 \rangle$ direction splits the band into two components associated with a characteristic polarization behavior. One component (shifting to lower energy) is observed for polarization of the incident light parallel to the $\langle 100 \rangle$ stress direction whereas the other one (shifting to higher energy) appears for perpendicular polarization. This splitting and polarization behavior is typical for a tetragonal center in a cubic crystal and in full accordance with the systematic theoretical

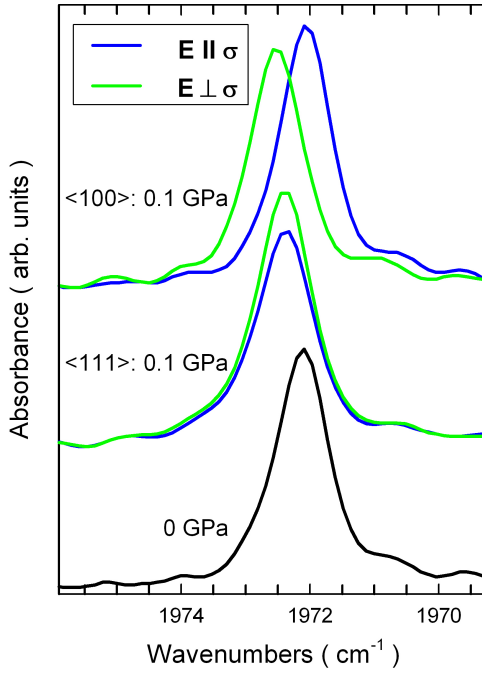


FIG. 2. Shift and splitting of the $[C_2N]_{As}$ absorption band at 1773 cm^{-1} band under stress in $\langle 100 \rangle$ and $\langle 111 \rangle$ direction at a sample temperature of 77 K.

TABLE I. Uniaxial stress characteristics of the 1773 and 2060 cm^{-1} bands in GaAs.

Direction of stress	Piezospectr. parameter	Intensity $I_{\parallel} : I_{\perp}$	Slope ($\text{cm}^{-1}/\text{GPa}$) 1773 cm^{-1}	2060 cm^{-1}
$\langle 100 \rangle$	A_1	1 : 0	-0.8	-0.2
	A_2	0 : 1	4	3.8
$\langle 111 \rangle$	$1/3(A_1 + 2A_2)$	1 : 1	2.4	2.5
$\langle 110 \rangle$	$1/2(A_1 + A_2)$	1 : 1	1.6	1.8

investigation of Kaplyanskii²⁴. The splitting is caused by lifting off the orientational degeneracy. It simply reflects the fact that a tetragonal center with its primary alignment along one of the three equivalent $\langle 100 \rangle$ directions has two possible orientations relative to the stress direction in the $\langle 100 \rangle$ case, however only one for the $\langle 111 \rangle$ stress case.

A summary of the results of the uniaxial stress experiments are given in FIG. 3 for $[C_2N]_{As}$ in (a) and $[CN_2]_{As}$ in (b). Measurements were carried out in the three crystallographic directions $\langle 100 \rangle$, $\langle 111 \rangle$, and $\langle 110 \rangle$ applying stress up to 0.125 GPa. Polarized measuring light with the electric field vector \vec{E} aligned parallel or perpendicular to the stress direction was used. For the $\langle 110 \rangle$ case, only one of the two branches was accessible due to the necessity of orienting the implanted layer perpendicular to the incident light (see section II). The piezospectroscopic parameters A_1 and A_2 according to Kaplyanskii's terminology²⁴ were derived from the fully polarized

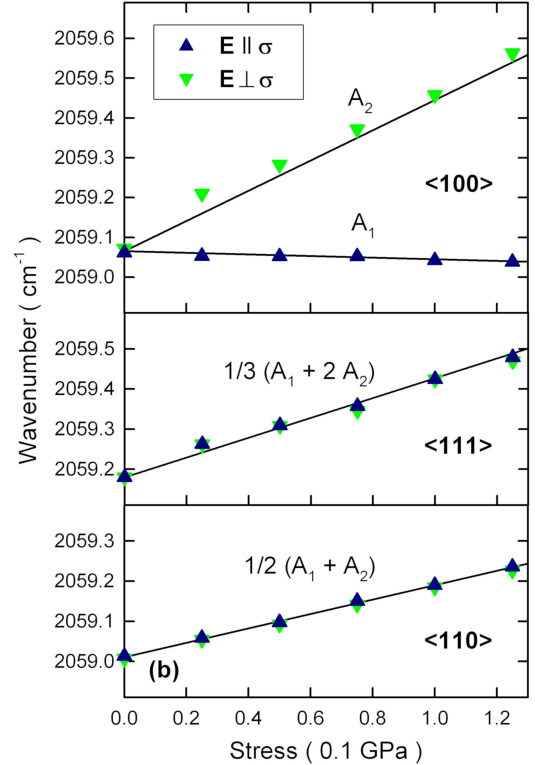
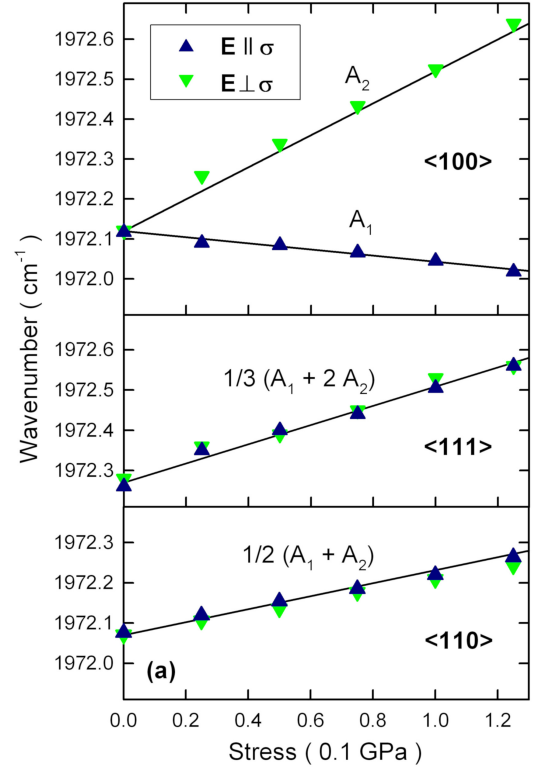


FIG. 3. Effect of uniaxial stress in $\langle 100 \rangle$, $\langle 111 \rangle$, and $\langle 110 \rangle$ directions on the frequency of the $[C_2N]_{As}$ (a) and the $[CN_2]_{As}$ band (b). Solid lines are fitted with piezospectroscopic parameters A_1 and A_2 . Sample temperature is 77 K.

TABLE II. Asymmetric stretching mode frequencies of the charged structures for ^{12}C and ^{14}N . d_{CC} is the bond length between two carbon atoms and d_{CN} between a carbon and a nitrogen atom.

Charge (e)	$[\text{CN}_2]_{\text{As}}$		$[\text{C}_2\text{N}]_{\text{As}}$		d_{CC} (\AA)
	ω (cm^{-1})	d_{CN} (\AA)	ω (cm^{-1})	d_{CN} (\AA)	
+2	2139.8	1.2204	2036.2	1.2403	1.2745
+1	2139.3	1.2201	-	1.2418	1.2718
0	2128.3	1.2206	2049.2	1.2414	1.2705
-1	2127.4	1.2210	-	1.2418	1.2713
-2	2122.3	1.2214	2042.0	1.2413	1.2718

branches for $\langle 100 \rangle$ stress. In the case of the 1973 cm^{-1} band, a complete fit of the experimental data is possible with $A_1 = -0.8\text{ cm}^{-1}/\text{GPa}$ and $A_2 = 4.0\text{ cm}^{-1}/\text{GPa}$. It should be mentioned that the peak position at zero stress shows some scattering between different samples, presumably due to residual strain in the implanted layer after annealing⁹. The results for the 2060 cm^{-1} band in (b) are shown for completeness. The piezospectroscopic parameters are within the experimental accuracy of about $\pm 10\%$ identical to the values obtained previously from bulk crystals⁸. This emphasizes the fact that the $[\text{CN}_2]_{\text{As}}$ center generated by implantation and RTA at $700\text{ }^\circ\text{C}$ is identical to the center observed in bulk crystals after long-term annealing at $700\text{ }^\circ\text{C}$ ¹⁰. Furthermore, the structural damage in the implanted layer and the high defect concentration obviously do not influence significantly the piezospectroscopic results. A compilation of all piezospectroscopic results is given in Table I.

The behavior under stress is similar for both carbon-nitrogen complexes in GaAs not only qualitatively but also quantitatively. It is also worth mentioning that the size of the parameters A_1 and A_2 is near to the values obtained by Ulrici and Clerjaud⁷ for the tetragonal carbon-nitrogen complex in GaP (2087 cm^{-1} band) indicating some similarities in bonding configuration. The negative sign of the parameter A_1 needs to be commented on. For $\langle 100 \rangle$ stress, this parameter reflects the response of the complex aligned with its axis parallel to the stress direction. Clearly, if the carbon-nitrogen bonds are compressed in this situation, the vibrational frequency should increase and A_1 should be positive. We will propose a model for this striking behavior in subsection III D.

C. Structural investigation and vibrational modes from DFT

Piezospectroscopy and its analysis strongly indicates that both complexes are aligned along the $\langle 100 \rangle$ directions of the GaAs crystal. The atomic configuration of the $[\text{CN}_2]_{\text{As}}$ and the $[\text{C}_2\text{N}]_{\text{As}}$ was chosen as N-C-N and C-C-N in a linear arrangement according to experimental results of subsections III A and III B. The structures after

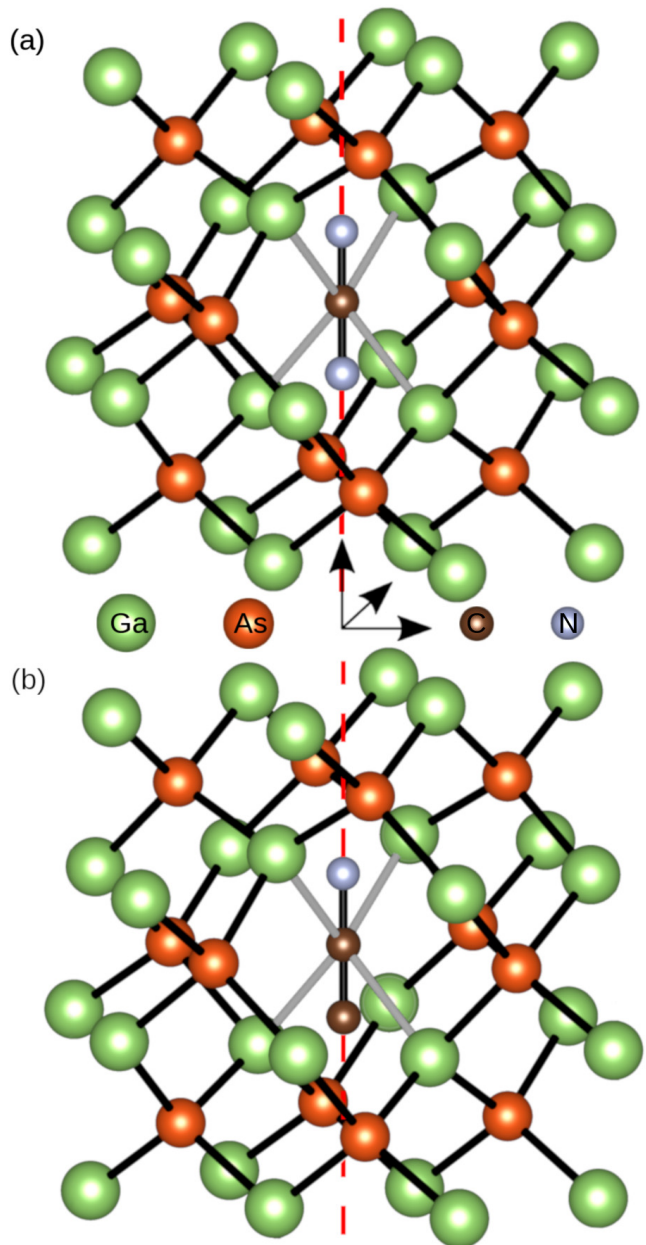


FIG. 4. Incorporation of the $[\text{CN}_2]_{\text{As}}$ (a) and the $[\text{C}_2\text{N}]_{\text{As}}$ (b) complex in GaAs. Both complexes are aligned along the $\langle 100 \rangle$ axes of the GaAs host crystal. The gray bonds indicate the actual bonds for a pure GaAs crystal to the removed As. Some surrounding atoms are removed for better representation breaking the periodic supercell used in the calculations.

relaxation are depicted in FIG. 4 for $[\text{C}_2\text{N}]_{\text{As}}$ in (a) and $[\text{CN}_2]_{\text{As}}$ in (b). The lattice constant amounts to 5.605 \AA for the defect-free GaAs crystal in comparison to the experimental 5.655 \AA . Although no symmetry constraints are applied to the DFT calculations, both defects are almost perfectly aligned along the $\langle 100 \rangle$ direction after the convergence is reached. Bond lengths of the complexes are documented in TAB. II.

Structures with a charge of $q = -3, \dots, +3$ were calcu-

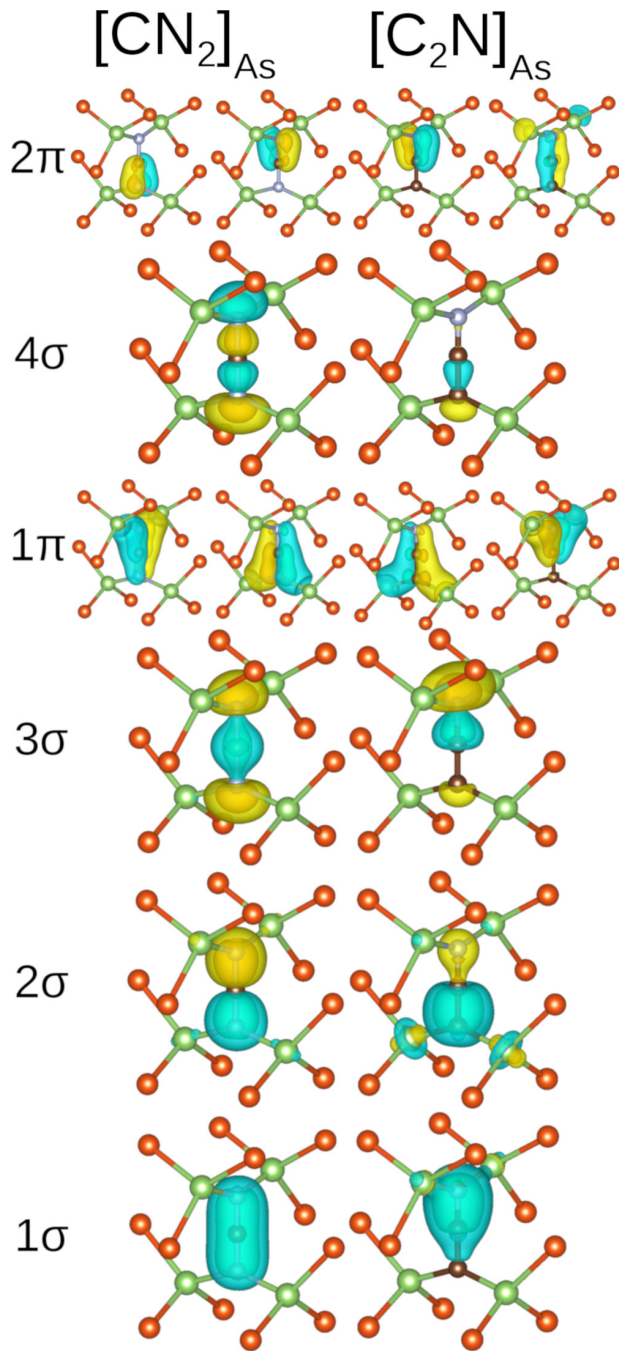


FIG. 5. Kohn-Sham molecular-like orbitals for $[\text{CN}_2]_{\text{As}}$ and $[\text{C}_2\text{N}]_{\text{As}}$ from HSE06 DFT calculations for different eigenvalues. The isosurfaces have the values ± 0.1 and $\pm 0.05/a_0^{-3/2}$ starting at the inner isosurface. Only strongly localized orbitals which are similar to the free molecule orbitals are shown.

lated by adding and removing electrons from the supercells. In this way the effect of a modified Fermi level on the occupation of states and resulting change of bonding forces was calculated. Surprisingly, the charged $[\text{CN}_2]_{\text{As}}$ and $[\text{C}_2\text{N}]_{\text{As}}$ structures remained in a symmetric configuration with almost unchanged bond length, contrary to

the case of the $[\text{CN}]_{\text{As}}$ complex as discussed by Limpijumong et al.¹². The calculation of the vibrational modes and their frequencies was carried out using the finite displacement²⁰ method with a displacement of $\pm 0.001\text{\AA}$ out of the equilibrium position for all atoms in the unit cell. To account for the effect of the lattice coupling on the LVM modes, we calculated the frequencies from the full dynamical matrix using the LDA approximation.

Inspection of the modes reveals that the highest frequency corresponds to the asymmetric and the second highest to the symmetric bond stretching mode. The third and fourth highest frequency are the two symmetry equivalent bending modes of the incorporated complex.²⁵

TAB. II shows the vibrational frequencies of the infrared active and asymmetric stretching modes for $[\text{CN}_2]_{\text{As}}$ and $[\text{C}_2\text{N}]_{\text{As}}$ in different charge states and the associated distance of the bond lengths. The change of the bond lengths is in the range of 0.1% to 0.01% accompanied by a similar small change of the frequency. An explanation for the small charge sensitivity of the vibrational modes is that electrons added or removed can not localize close to the carbon-nitrogen complex since no defect states are available in the band gap, see III E for further discussion. It should be noted, that the vibrational frequencies are calculated within the LDA approximation which is known to overestimate the delocalization of the electrons due to a self-interaction error. This error may decrease the variation of the bond length for different charges unphysically.

The vibrational frequencies for the carbon-nitrogen complexes in an isotopic configuration were calculated by substituting the masses in the dynamical matrix. Subsequently, the vibrational frequencies were obtained by diagonalization of the modified eigenvalue equation. TAB. III and IV show the frequencies of the asymmetric stretching modes (highest frequency) for the $[\text{CN}_2]_{\text{As}}$ and $[\text{C}_2\text{N}]_{\text{As}}$ complexes in comparison to the assigned frequencies from the infrared measurements. To eliminate a systematic error of DFT and the neglect of anharmonic effects, a scaling factor $\sum_i \omega_{\text{calc}} \omega_{\text{exp}} / \sum_i \omega_{\text{calc}}^2$ for the frequency is introduced according to Ref. 26. The factor corrects the average of the frequencies of the mass multiplet less than 4%. For both complexes the frequencies of the mass multiplets from experiment and DFT agree very well within 1 cm^{-1} . This excellent agreement strongly supports the hypothesis that the measured vibrational modes are generated by the here presented $[\text{CN}_2]_{\text{As}}$ and $[\text{C}_2\text{N}]_{\text{As}}$ complexes.

D. Kohn-Sham molecular-like orbitals and bonding to the lattice

The calculated weak dependence of the asymmetric stretching mode on the supercell charge is comprehensible when the added or subtracted electrons do not occupy energy levels relevant for the bonds in the carbon-nitrogen complex. On the other hand, missing this de-

TABLE III. Comparison of the asymmetric stretching mode frequency of neutral $[\text{CN}_2]_{\text{As}}$ in different isotopic configurations between experiment (c.f. FIG. 1) and theory. The scaling factor is 0.9679. Numbers marked with * are from samples implanted with ^{15}N in presence of ^{12}C measured at 77 K (Ref. 9). Numbers in brackets are the prediction for a possible experiment implanting ^{15}N together with ^{13}C .

C	N ₁	N ₂	ω_{calc} (cm^{-1})	ω_{scaled} (cm^{-1})	ω_{exp} (cm^{-1})
12	14	14	2128.3	2060.0	2059.6
12	14	15	2118.0	2050.0	2050*
12	15	15	2107.4	2039.8	2040*
13	14	14	2069.7	2003.3	2003.7
13	14	15	2059.1	1993.0	(1993)
13	15	15	2048.1	1982.4	(1982)

TABLE IV. Comparison of the asymmetric stretching mode frequency of neutral $[\text{C}_2\text{N}]_{\text{As}}$ in different isotopic configurations between experiment (see FIG. 1) and theory. The scaling factor is 0.9629

C ₁	C ₂	N	ω_{calc} (cm^{-1})	ω_{scaled} (cm^{-1})	ω_{exp} (cm^{-1})
12	12	14	2049.2	1973.1	1972.7
12	13	14	2034.9	1959.3	1958.4
13	12	14	1994.5	1920.4	1921.4
13	13	14	1979.7	1906.2	1906.5

pendence, the charge of the complexes cannot be deduced by simple comparison between measured and calculated vibrational frequencies.

To confirm this observation and to identify the charge of the complexes we further investigated the electronic structure. Since LDA is known to produce an inadequate picture of Kohn-Sham (KS) eigenvalues and especially of band gaps, we used the HSE06 hybrid functional to find the minimum of energy with atomic positions fixed at the final LDA positions. It turned out that a few of the KS orbitals are spatially localized around the complexes and resemble molecular-like orbitals of a free N-C-N and a C-C-N molecule. KS orbitals of the free molecules can be found in the Supplementary Material in FIG. S1 and S2.

For the neutral N-C-N free molecule with 14 valence electrons molecular-orbital theory predicts, analogous to the case of the CO_2 , the orbitals $(1\sigma_g)^2$, $(1\sigma_u)^2$, $(2\sigma_g)^2$, $(1\pi_u)^4$, $(2\sigma_u)^2$, and $(1\pi_g)^2$ (partially occupied) as bonding and non-bonding, followed by further unoccupied antibonding orbitals. On the other hand, neutral C-C-N free molecule with 13 valence electrons gives rise to similar orbitals labeled with σ and π . Since the C-C-N molecule has a linear, internuclear axis and the inversion symmetry is missing, no parity assignment are necessary. To compare localized KS molecular-like orbitals of $[\text{CN}_2]_{\text{As}}$ with $[\text{C}_2\text{N}]_{\text{As}}$ and with KS molecular orbitals from the free N-C-N and C-C-N molecules, we rename the above orbitals to 1σ , 2σ , 3σ , 1π , 4σ , and 2π . The

TABLE V. Localized molecular-like orbitals of $[\text{CN}_2]_{\text{As}}$ and $[\text{C}_2\text{N}]_{\text{As}}$, their energy relative to the VBM and the assignment of charges to the two gallium atoms $q_{2\text{Ga}}$, the nitrogen atom q_{N} and the carbon atom q_{C} according to the Mulliken analysis. Note, the splitting of the degenerated π orbitals for $[\text{C}_2\text{N}]_{\text{As}}$ case.

$[\text{CN}_2]_{\text{As}}$	E (eV)	$q_{2\text{Ga}}$	q_{N}	q_{C}	q_{N}	$q_{2\text{Ga}}$
$2\pi^4$	-5.8	0.01	0.19	0.09	0.01	0.16
$4\sigma^2$	-8.4	0.07	0.26	0.11	0.26	0.07
$1\pi^4$	-8.9	0.14	0.34	0.23	0.09	0.00
$3\sigma^2$	-9.3	0.06	0.30	0.10	0.30	0.06
$2\sigma^2$	-20.5	0.07	0.37	0.10	0.37	0.07
$1\sigma^2$	-22.6	0.01	0.29	0.41	0.29	0.01
$[\text{C}_2\text{N}]_{\text{As}}$	E (eV)	$q_{2\text{Ga}}$	q_{N}	q_{C}	q_{C}	$q_{2\text{Ga}}$
$2\pi^2$	-5.2	0.16	0.05	0.10	0.05	0.05
$2\pi^2$	-5.5	0.02	0.26	0.13	0.00	0.13
$4\sigma^2$	-7.5	0.01	0.01	0.02	0.06	0.08
$1\pi^2$	-7.9	0.00	0.07	0.02	0.18	0.22
$1\pi^2$	-8.6	0.21	0.35	0.14	0.02	0.00
$3\sigma^2$	-8.6	0.14	0.49	0.10	0.05	0.03
$2\sigma^2$	-15.5	0.03	0.06	0.25	0.40	0.22
$1\sigma^2$	-21.2	0.10	0.62	0.29	-0.01	-0.01

integer labels the energy in ascending order. The electron occupation in the crystal is not partial as in the free molecule but turns out to be maximal, adopting the electrons from the surrounding Ga. Not considered are the six 1s core electrons heavily bound in three σ orbitals.

The orbitals strongly localized around the complexes were identified by selecting the KS orbitals with sufficiently large localization on a C or N atom measured by means of the Mulliken charges ($q > 0.1$). Furthermore, the KS orbitals of the free complexes are taken into account for the identification. The $|\psi| = 0.05$ and $0.1 \text{ a}_0^{-3/2}$ isosurfaces for $[\text{CN}_2]_{\text{As}}$ and $[\text{C}_2\text{N}]_{\text{As}}$ are shown in FIG. 5 with the associated energies and charges of the participating atoms in TAB. V. The KS orbitals of the free N-C-N and C-C-N molecules are shown in the Supplementary Material in FIG. S1 and S2.

The localized orbitals of the complexes in GaAs are very similar to the orbitals of the molecule but extent for some eigenstates over the neighbouring Ga atoms, indicating the order of magnitude of bonding to the surrounding GaAs crystal. A Mulliken charge analysis helps to identify the bond structure inside the complexes and is depicted in TAB. V. Note that the charges of the lower orbitals sum up to nearly one and the charges of the higher orbitals to less than one, indicating an increasing delocalization of the KS orbitals and vice versa. The Mulliken charges for $[\text{C}_2\text{N}]_{\text{As}}$ show a significant asymmetry resulting from the stronger electronegativity of N compared to C. Among these orbitals, the largest charge at the neighbouring Ga atoms is for the 1π orbital. It is suspected that this orbital gives the largest contribution to the bond between the N-C-N and C-C-N complex and the crystal.

From the Mulliken charge distribution, the strength

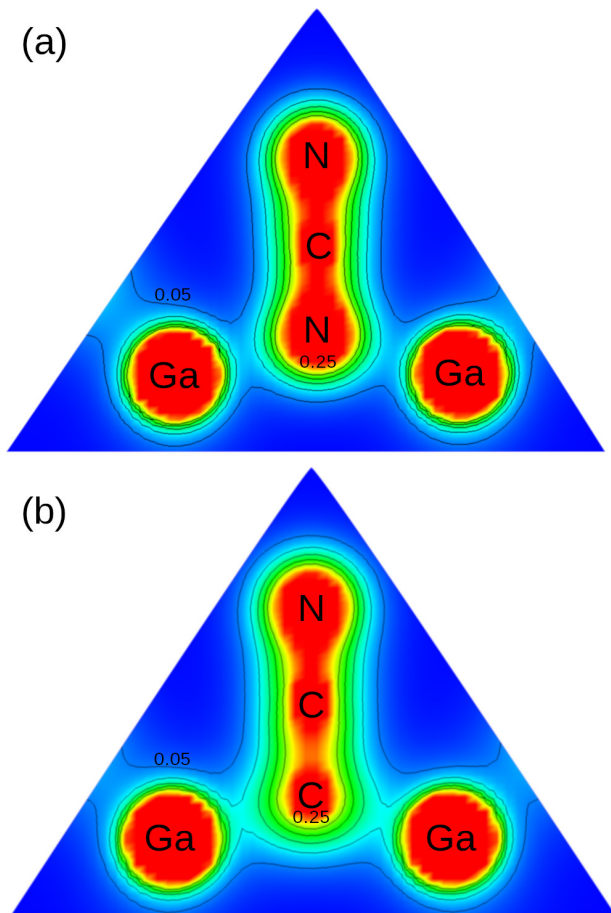


FIG. 6. Full electron density of $[\text{CN}_2]_{\text{As}}$ (a) and $[\text{C}_2\text{N}]_{\text{As}}$ (b) in units of e/a_0^3 . The values of the contour lines are equidistant beginning with $0.05 e/a_0^3$ and ending with $0.25 e/a_0^3$.

of a bond cannot be unambiguously concluded. To support the statement about the 1π orbital as the major bond from the carbon-nitrogen complex to the surrounding GaAs crystal, a 2D section of the full electron density around the complex is shown in FIG. 6. The 2D section of (a) is aligned to the Ga-N-Ga plane and of (b) to the Ga-C-Ga plane. In comparison to the single orbitals, the full electron density includes all orbitals and thus is more suitable for bond strength analysis. Since the electron density between C-N and C-C is much higher than the electron density to the surrounding Ga atoms in FIGs. 6 (a) and (b), it can be concluded that the carbon-nitrogen complex can vibrate largely independently from the lattice, leading to the characteristics of a molecular-like LVM.

Furthermore, a closer inspection of the electron density in FIG. 6 reveals the Ga-C bond to be stronger than the Ga-N bond. A chemical explanation may be, the smaller electronegativity of the C compared to the N which allows the Ga to collect more electron density for the Ga-C bond than for the Ga-N bond. Consequently, the C-C-N entity is overall stronger bonded to the crystal than the N-C-N entity.

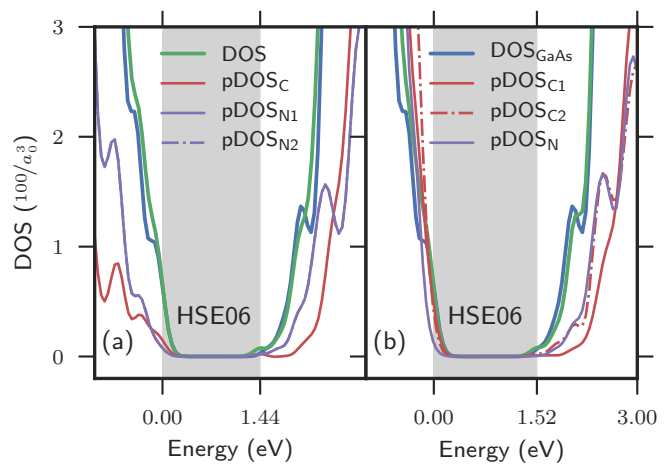


FIG. 7. Density of states (DOS) and the projected density of states (pDOS) of the C (pDOS_C) and N (pDOS_N) atom of the complex from HSE06 functional calculations are portrayed for the $[\text{CN}_2]_{\text{As}}$ and $[\text{C}_2\text{N}]_{\text{As}}$ complex in (a) and (b), respectively. DOS_{GaAs} is the density of states for the pure GaAs host crystal. The DOS and DOS_{GaAs} are scaled by $1/200$

The above analyses of the molecular-like orbitals and the resulting bonding situation in the GaAs host lattice now allow a qualitative interpretation of the piezospectroscopic results. The linear N-C-N and C-C-N entities form valence bonds with the lattice only between the end atoms (N or C) and the (two) nearest-neighbour Ga atoms. The bond angles in the neutral charge state amount to 147.5° for $[\text{CN}_2]_{\text{As}}$ (Ga-N-Ga) and 144.9° for $[\text{C}_2\text{N}]_{\text{As}}$ (both Ga-C-Ga and Ga-N-Ga). In the sense of the discussion above and the charge-density result plotted in FIG. 6, we can treat the complexes approximately as a rigid unit. When applying stress in a $\langle 100 \rangle$ direction, the lattice is compressed in this direction and the bond angles become larger for those complexes oriented parallel to the stress direction. Therefore, the supporting action of the bonds decreases, inducing a slight downshift of the asymmetric stretching mode frequency. This is the reason for the negative sign of the piezospectroscopic parameter A_1 (see TAB. I). On the other hand, for those complexes oriented perpendicular to the stress direction, bond angles will decrease and the frequency increase. Consequently, the parameter A_2 will be positive.

E. Formation energies

After clarifying the charge environment of the complexes, and the strength and positions of the bonds, the actual charge state of the complexes remains to be discussed. This property is determined from the energy levels inside the band gap, close to valence and conduction band edges, and their occupation (Fermi level). To answer this question the use of the HSE06 hybrid functional for the electronic structure is essential because of the

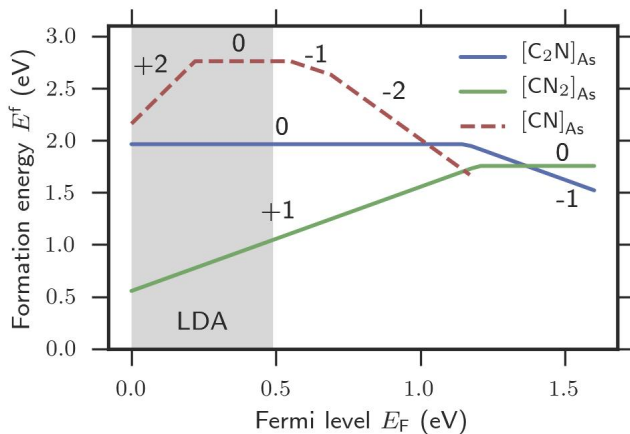


FIG. 8. Formation energies are calculated according to EQ. 1 except $[\text{CN}]_{\text{As}}$ which is from Ref. 12. The gray shaded area indicates the band gap calculated with the LDA functional.

smaller model uncertainty compared to the LDA functional. The band gaps from LDA (HSE06) DFT calculations were 0.49 eV (1.57 eV), 0.42 eV (1.44 eV) and 0.49 eV (1.52 eV) for GaAs, and the centers $[\text{CN}_2]_{\text{As}}$ and $[\text{C}_2\text{N}]_{\text{As}}$, respectively. The experimental band gap of GaAs is ≈ 1.52 eV. The LDA functional calculations highly underestimate the experimental band gap and the HSE06 calculations provide a value close to the experimental gap.

To find potential thermodynamic charge transition levels established by the $[\text{CN}_2]_{\text{As}}$ or $[\text{C}_2\text{N}]_{\text{As}}$ complexes, we have calculated the density of states (DOS) and the projected density of states (pDOS) of the C (pDOS_C) and N (pDOS_N) atoms. The energies of the DOS and pDOS in FIG. 7 are aligned to its relative VBM and show no defect levels in the band gap for both carbon-nitrogen complexes. Although this observation gives a hint, regarding the fact that the hybrid functionals often give good results for the electronic structure, it is not compelling.

Therefore, we have calculated the formation energy as a function of the Fermi energy using the HSE06 hybrid functional according to EQ. 1. Fig. 8 shows the Fermi energy dependent formation energies for both complexes in different charge states. Since only charge states with the lowest formation energy are drawn, the kinks indicate the thermodynamic charge transition levels. The charge transition levels were calculated using LDA structural energies and were aligned using the HSE06 VBM with respect to the average electrostatic potential according to Ref. 27.

For comparison, we have inserted the formation energy of the proposed $[\text{CN}]_{\text{As}}$ complex as calculated by Limpitjumnong et al.¹². In general, the formation energy of the $[\text{CN}_2]_{\text{As}}$ and $[\text{C}_2\text{N}]_{\text{As}}$ complex in GaAs are lower than the $[\text{CN}]_{\text{As}}$ complex, revealing them more likely. Furthermore, the formation energy of the $[\text{CN}_2]_{\text{As}}$ complex

is lower than of $[\text{C}_2\text{N}]_{\text{As}}$ for almost the entire band gap. This coincides with the experimental observation that the vibrational frequency attributed for the $[\text{CN}_2]_{\text{As}}$ center can be found in bulk GaAs whereas the signature of $[\text{C}_2\text{N}]_{\text{As}}$ is only found in implanted samples.

The charge transition levels $\epsilon(+1/0) = 1.18$ eV for $[\text{CN}_2]_{\text{As}}$ and $\epsilon(0/-1) = 1.15$ eV for $[\text{C}_2\text{N}]_{\text{As}}$ are both located in a distance to the conduction band minimum (CBM) at 1.52 eV and, therefore, could be interpreted as deep defects. On the other hand, for both the $[\text{CN}_2]_{\text{As}}$ and $[\text{C}_2\text{N}]_{\text{As}}$ complexes, no KS defect levels could be found inside the band gap, neither from LDA nor from HSE06 calculations, but only levels very close to the CBM (cf. FIG. 7).

The results of both approaches to identify the thermodynamic charge transition levels and its associated charges are inconsistent on a certain level of accuracy. The DOS approach is limited because it considers KS orbitals, the formation energy approach is limited because it contains LDA energies and several correction terms. We conjecture that the charge transition level for both carbon-nitrogen complexes should actually move exactly to the CBM if calculated in a larger supercell and with even more accuracy provided by a still higher level of theory. When the charge transition levels are exactly at the CBM, the $[\text{C}_2\text{N}]_{\text{As}}$ complex is neutral and the $[\text{CN}_2]_{\text{As}}$ defect is positively charged for a regular Fermi energy.

IV. CONCLUSION

The carbon-nitrogen complexes $[\text{CN}_2]_{\text{As}}$ and $[\text{C}_2\text{N}]_{\text{As}}$ form stable molecular-like complexes in GaAs. Piezospectroscopic FTIR investigations on the associated vibrational absorption bands at 2060 cm^{-1} for $[\text{CN}_2]_{\text{As}}$ and 1973 cm^{-1} for $[\text{C}_2\text{N}]_{\text{As}}$ prove that both complexes have tetragonal symmetry with the axis oriented parallel to the $\langle 100 \rangle$ direction.

The geometry prediction of the complexes from FTIR investigations was used to carry out DFT calculations. After geometry relaxation, the structure from DFT stayed in the predicted structure and, hence, substantiate the experimental investigation. Furthermore, vibrational frequencies of the highest and asymmetric stretching mode for both complexes are within a few wave numbers with the FTIR measurements including band shifts due to isotopes.

The $[\text{CN}_2]_{\text{As}}$ in GaAs complex is the structural analogue to the linear CO_2 molecule. In accordance with piezospectroscopic results, the substitutional position with the C atom on the anion site (As) and the N-C-N or C-C-N axis oriented along the $\langle 100 \rangle$ direction has lowest energy. The change of bond lengths and, consequently, the frequencies of the asymmetric stretching mode of both complexes with the charge state are relatively small.

The portrayed structural model for the complexes explains the negative piezospectroscopic parameter A_1 from

the FTIR measurements. In addition, a detailed inspection of electronic charge density is consistent with the larger absolute value of A_1 of $[\text{C}_2\text{N}]_{\text{As}}$ compared to $[\text{CN}_2]_{\text{As}}$.

Concluding the formation energies, the $[\text{CN}_2]_{\text{As}}$ complex is more stable than the $[\text{C}_2\text{N}]_{\text{As}}$ complex and a possible $[\text{CN}]_{\text{As}}$ complex is less likely. The most likely charge state assignment for $[\text{CN}_2]_{\text{As}}$ is singly positive (1+) and for $[\text{C}_2\text{N}]_{\text{As}}$ neutral (0). This results from an interpretation of the density of states and the formation energies.

Altogether, the consistency between experimental results and first-principles calculations in this study is excellent.

SUPPLEMENTARY MATERIAL

See supplementary material for the CN_2 and C_2N KS molecular-like orbitals from HSE06 DFT calculations.

ACKNOWLEDGMENTS

The authors are indebted to W. Ulrici for helpful discussions and to U. Kretzer from Freiburger Compound Materials, Freiberg, Germany, for the supply of high-purity GaAs materials. The work was funded in part by the Deutsche Forschungsgemeinschaft (DFG). The authors gratefully acknowledge the Gauss Centre for Supercomputing e.V. (www.gauss-centre.eu) for funding this project by providing computing time on the GCS Supercomputer SuperMUC at Leibniz Supercomputing Center (LRZ, www.lrz.de).

- ¹M. Jurisch, F. Börner, T. Bünger, S. Eichler, T. Flade, U. Kretzer, A. Köhler, J. Stenzenberger, and B. Weinert, *J. Cryst. Growth* **275**, 283 (2005).
- ²K. Saito, E. Tokumitsu, T. Akatsuka, M. Miyauchi, T. Yamada, M. Konagai, and K. Takahashi, *J. Appl. Phys.* **64**, 3975 (1988).
- ³C. R. Abernathy, S. J. Pearton, R. Caruso, F. Ren, and J. Kovalchik, *Appl. Phys. Lett.* **55**, 1750 (1989).
- ⁴M. Weyers, M. Sato, and H. Ando, *Jpn. J. Appl. Phys.* **31**, L853 (1992).
- ⁵D. B. Jackrel, S. R. Bank, H. B. Yuen, M. A. Wistey, J. S. Harris, A. J. Ptak, S. W. Johnston, D. J. Friedman, and S. R. Kurtz, *J. Appl. Phys.* **101**, 114916 (2007).
- ⁶A. Polimeni, G. H. Baldassarri, M. Capizzi, G. B. H. ger von H gersthal, M. Bissiri, A. Frova, M. Fischer, M. Reinhardt, A. Forchel, and G. B. H. von Hogersthal, *Semicond. Sci. Technol.* **17**, 161 (2002).
- ⁷W. Ulrici and B. Clerjaud, *Phys. Rev. B - Condens. Matter Mater. Phys.* **72**, 045203 (2005).
- ⁸H. C. Alt, A. Kersch, and H. E. Wagner, *Phys. Status Solidi Basic Res.* **250**, 324 (2013).
- ⁹H. C. Alt, H. E. Wagner, A. Glacki, C. Frank-Rotsch, and V. Haeublein, *Phys. Status Solidi Basic Res.* **252**, 1827 (2015).
- ¹⁰W. Ulrici and M. Jurisch, *Phys. Status Solidi Basic Res.* **242**, 2433 (2005).
- ¹¹H. C. Alt, B. Wiedemann, and K. Bethge, *Mater. Sci. Forum* **258-263**, 867 (1997).
- ¹²S. Limpijumnong, P. Reunchan, A. Janotti, and C. G. Van De Walle, *Phys. Rev. B - Condens. Matter Mater. Phys.* **77** (2008), 10.1103/PhysRevB.77.195209.
- ¹³V. Blum, R. Gehrke, F. Hanke, P. Havu, V. Havu, X. Ren, K. Reuter, and M. Scheffler, *Comput. Phys. Commun.* **180**, 2175 (2009).
- ¹⁴F. Knuth, C. Carbogno, V. Atalla, V. Blum, and M. Scheffler, *Comput. Phys. Commun.* **190**, 33 (2015).
- ¹⁵A. Marek, V. Blum, R. Johanni, V. Havu, B. Lang, T. Auckenthaler, A. Heinecke, H.-J. Bungartz, and H. Lederer, *J. Phys. Condens. Matter* **26**, 213201 (2014).
- ¹⁶T. Auckenthaler, V. Blum, H. J. Bungartz, T. Huckle, R. Johanni, L. Krämer, B. Lang, H. Lederer, and P. R. Willems, *Parallel Comput.* **37**, 783 (2011).
- ¹⁷V. Havu, V. Blum, P. Havu, and M. Scheffler, *J. Comput. Phys.* **228**, 8367 (2009).
- ¹⁸J. P. Perdew and Y. Wang, *Phys. Rev. B* **45**, 13244 (1992), arXiv:arXiv:1011.1669v3.
- ¹⁹X. Ren, P. Rinke, V. Blum, J. Wieferink, A. Tkatchenko, A. Sanfilippo, K. Reuter, and M. Scheffler, *New J. Phys.* **14** (2012), 10.1088/1367-2630/14/5/053020, arXiv:1201.0655.
- ²⁰A. Togo and I. Tanaka, *Scr. Mater.* **108**, 1 (2015), arXiv:1506.08498.
- ²¹C. Freysoldt, B. Grabowski, T. Hickel, J. Neugebauer, G. Kresse, A. Janotti, and C. G. Van De Walle, *Rev. Mod. Phys.* **86**, 253 (2014).
- ²²K. Momma and F. Izumi, *J. Appl. Crystallogr.* **44**, 1272 (2011).
- ²³For simplicity we keep the terminology 1973 and 2060 cm^{-1} band throughout the paper, although at 77 K and in some implanted layers the peak position is closer to 1972 and 2059 cm^{-1} , respectively.
- ²⁴A. A. Kaplyanskii, *Opt. Spectrosc.* **16** (1964).
- ²⁵The third and fourth highest vibrational mode (bending) could not be measured by FTIR experiments. Although the vibrational modes should be IR-active from symmetry, we assume that the oscillator strength is not high enough for detection.
- ²⁶K. K. Irikura, R. D. Johnson, and R. N. Kacker, *J. Phys. Chem. A* **109**, 8430 (2005).
- ²⁷R. Ramprasad, H. Zhu, P. Rinke, and M. Scheffler, *Phys. Rev. Lett.* **108**, 066404 (2012).